

Vortex Interactions and Thermally Induced Crossover from Type-I to Type-II Superconductivity

J. Hove,^{*} S. Mo,[†] and A. Sudbø[‡]

Department of Physics
Norwegian University of Science and Technology,
N-7491 Trondheim, Norway

(Dated: October 24, 2018)

We have computed the effective interaction between vortices in the Ginzburg-Landau model from large-scale Monte-Carlo simulations, taking thermal fluctuations of matter fields and gauge fields fully into account close to the critical temperature. We find a change, in the form of what appears to be a crossover, from an attractive to a repulsive effective vortex interactions in an intermediate range of Ginzburg-Landau parameters $\kappa \in [0.76, 1]/\sqrt{2}$ upon increasing the temperature in the superconducting state. This corresponds to a thermally induced crossover from type-I to type-II superconductivity around a temperature $T_{Cr}(\kappa)$, which we map out in the vicinity of the metal-to-superconductor transition. In order to see this crossover, it is essential to include amplitude fluctuations of the matter field, in addition to phase-fluctuations and gauge-field fluctuations. We present a simple physical picture of the crossover, and relate it to observations in Ta and Nb elemental superconductors which have low-temperature values of κ in the relevant range.

PACS numbers: 74.55.+h, 74.60.-w, 74.20.De, 74.25.Dw

I. INTRODUCTION

The nature of the phase-transition in systems of a scalar matter field coupled to a massless gauge-field has a long history in condensed matter physics, dating at least back to the introduction of the Ginzburg-Landau (GL) theory of superconductivity¹. At the mean-field level, ignoring spatial variations in gauge fields as well as matter fields leads to the prediction of a second order phase transition in the model, with classical mean-field exponents for all values of the GL parameter κ . The first attempt to seriously consider the role of fluctuations on the order of the metal-to-superconductor transition was made by Halperin, Lubensky, and Ma², who found that ignoring matter-field fluctuations entirely, and treating gauge-field fluctuations exactly, resulted in a permanent first order transition for all values of κ , since the gauge-field-fluctuations produced an extra term $\sim -|\phi|^3$ in the matter field sector of the theory in three spatial dimensions, where the complex matter field is denoted by ϕ and represents the condensate order parameter. (In the context of particle physics, Coleman and Weinberg³ studied the equivalent problem of spontaneous symmetry breaking due to radiative corrections in the Abelian Higgs model in four space-time dimensions, finding the additional term $\phi^4 \ln(\phi^2/\phi_0^2)$, where the real matter field is denoted ϕ and represents a scalar meson.)⁴ Subsequently, Dasgupta and Halperin⁵ found, using duality arguments in conjunction with Monte-Carlo simulations, that when gauge-field fluctuations and phase fluctuations

of the scalar matter field are taken into account, but amplitude fluctuations are ignored, the phase transition is permanently second order⁵. Bartholomew⁶ then reported results from Monte-Carlo simulations for the case when also amplitude fluctuations are taken into account, concluding that the phase transition changes from first to second order at a particular value of the GL parameter $\kappa \approx 0.4/\sqrt{2}$. As far as this numerical value is concerned, note that the problem of finding a *tricritical* value κ_{tri} separating first and second order transitions is extremely demanding even by present day supercomputing standards⁷ (see below). Using ingenious duality arguments, Kleinert⁸ obtained that the change from first to second order transition should occur at $\kappa \approx 0.8/\sqrt{2}$. The value of κ that separates a first order (discontinuous) transition from a second order (continuous) one, defines a tricritical point⁹, and will hereafter be denoted κ_{tri} . Note that to obtain the above result, it is necessary to allow for amplitude fluctuations in the superconducting order parameter, which become important for small to intermediate values of κ , but are totally negligible in the extreme type-II regime $\kappa \gg 1$.

The critical properties of a superconductor may be investigated at the phenomenological level by the GL model of a complex scalar matter field ϕ coupled to a fluctuating massless gauge field \mathbf{A} . It is this feature of the gauge field that makes the GL model so difficult to access by the standard techniques employing the renormalisation group^{2,11}. The GL model in d spatial dimensions is defined by the functional integral

$$Z = \int \mathcal{D}A_\nu \mathcal{D}\phi \exp\left[-\int d^d x \left[\frac{1}{4} F_{\mu\nu}^2 + |(\partial_\nu + iqA_\nu)\phi|^2 + m^2|\phi|^2 + \lambda|\phi|^4 \right] \right] \quad (1)$$

where $F_{\mu\nu} = \partial_\mu A_\nu - \partial_\nu A_\mu$, q is the charge coupling the condensate matter field ϕ to the fluctuating gauge field A_μ , λ is a self coupling, and m^2 is a mass parameter which changes sign at the mean field critical temperature. When all dimensionful quantities are expressed in powers of the scale represented by q^2 , the GL model may be formulated in terms of the two dimensionless parameters $y = m^2/q^4$ and $x = \lambda/q^2$. In this case, y is temperature like and drives the system through a phase transition, and $x = \kappa^2$ is the square of the Ginzburg-Landau parameter. Depending on the value of x , the transition is either first order for $x < x_{\text{tri}}$, or continuous for $x > x_{\text{tri}}$ ^{6,7,8}.

In a recent paper⁷, we have determined $x_{\text{tri}} = 0.295 \pm 0.025$. This corresponds to a tricritical value of the GL parameter $\kappa_{\text{tri}} = (0.76 \pm 0.04)/\sqrt{2}$, in rather remarkable agreement with the results of Ref. 8. *Moreover in Ref. 7 it was also argued that this value of x or κ is the demarkation value which separates type-I and type-II superconductivity, rather than the classical mean-field value $\kappa = 1/\sqrt{2}$.* The connection can be made when one realizes that *criticality* at the metal-to-superconductor transition requires that topological defects of the matter field in the form of vortex loops are stable. On the other hand, there is a connection between critical exponents and geometric properties of a tangle of such vortex loops¹⁴. The fractal dimension D_H of the vortex-loop tangle is connected to the anomalous scaling dimension η_ϕ ¹³ of the matter field in a field theory of the vortex-loop gas, a theory dual to the original GL theory^{12,13} by the relation $D_H + \eta_\phi = 2$. Since the anomalous scaling dimension is connected to the order parameter exponent β of the dual matter field by the relation $2\beta = \nu(d - 2 + \eta_\phi)$ ^{13,14}, it follows that a collapse of the vortex-loop tangle implies $D_H = d$ and hence $\beta = 0$ indicative of a first order transition. Here, d is the spatial dimension of the system. Now, a collapse of the tangle in turn implies an effective attraction between vortices, or type-I behavior. On the other hand, a stable vortex-loop tangle at the critical point, with fractal dimension $D_H < d$, implies first of all type-II behavior, but also $\eta_\phi > 2 - d$ and $\beta > 0$, and hence a second order transition.

The above assertion, that the tricritical value of κ separates first order from second order metal-to-superconductor transition, and moreover also separates type-I from type-II behavior when the system is on the phase-transition line $y_c(x)$, is in contrast to the conventional wisdom that type-I and type-II superconductivity is separated by $x = 0.5$. Based on the above arguments, we have proposed the phase diagram shown in Fig. 1 of Ref. 7 which contains a new line separating type-I and type-II superconductivity. The shape of this line was inferred from the observation that far from the

phase transition, mean-field estimates of the boundary between type-I and type-II should be precise, and hence this boundary should asymptotically approach $x = 0.5$ from below as the temperature is reduced.

It is the purpose of this paper to show directly, by computing the effective thermally renormalized interaction between vortices via large-scale Monte-Carlo simulations, that this quantity changes from being repulsive to attractive in the intermediate regime $\kappa \in [0.76, 1]/\sqrt{2}$. Since the sign of the vortex-interaction is the microscopic diagnostics, in terms of vortex degrees of freedom, for distinguishing type-I from type-II superconductivity, the large-scale simulations we present in this paper confirm the above conjectures and plausibility arguments of Ref. 7.

In an external field the GL model has classical solutions in terms of Abrikosov flux tubes¹⁵, or Nielsen-Olesen vortices¹⁶, and the concept of type-I versus type-II superconductivity is based on the interaction between these vortices. For type-I superconductors they attract each other, whereas for type-II superconductors the interaction is repulsive. Abrikosov¹⁵ showed that at the *mean field* level type-I and type-II superconductors are separated at $\kappa = 1/\sqrt{2}$. We will refer to the value of κ separating type-I from type-II behavior at $\kappa_{\text{I/II}}$, which we find varies with y . It is not a sharply defined quantity, since it represents a crossover line. The exception is at $y = y_c, x = x_{\text{tri}}$, where $\kappa_{\text{I/II}} = \kappa_{\text{tri}}$. Elaborate calculations of vortex interactions have been carried out^{17,18,19,20,21}, but none of these approaches take thermal fluctuations into account. A recent overview of superconductors with κ close to $1/\sqrt{2}$ can be found in Ref. 22, see also Ref. 23.

Superconductors with $\kappa \approx 1/\sqrt{2}$ were studied extensively in the 1960s and 1970s²², and in particular measurements on the metals Ta and Nb demonstrated that the notion of a *temperature independent* value of $\kappa_{\text{I/II}}$ was incorrect²⁴. At the time, this was explained with a mean-field theory involving three GL parameters²⁵. Thermal fluctuations, not addressed at the mean-field level, offer an alternative and above all simpler explanation for the observations of crossovers from type-I to type-II behavior in one and the same compound as the temperature is increased.

We have performed large scale Monte Carlo (MC) simulations on the lattice version of Eq. 1, with two vortices penetrating the sample in the \hat{z} direction. By measuring the interaction between these two vortices we have determined the value of $\kappa_{\text{I/II}}$, in particular how this value is affected by thermal fluctuations close to the critical point.

II. MODEL, SIMULATIONS AND RESULTS

To perform simulations on Eq. 1, we have defined a discrete version as follows²⁷:

$$Z = \int \mathcal{D}\boldsymbol{\alpha} \mathcal{D}\psi \exp(-S[\boldsymbol{\alpha}, \psi])$$

$$S[\boldsymbol{\alpha}, \psi] = \beta_G \sum_{\mathbf{x}, i < j} \frac{1}{2} \alpha_{ij}(\mathbf{x})^2 - \frac{2}{\beta_G} \sum_{\mathbf{x}, i} \text{Re} \left[\psi^*(\mathbf{x}) e^{i\alpha_i(\mathbf{x})} \psi(\mathbf{x} + \hat{i}) \right] + \beta_2 \sum_{\mathbf{x}} \psi^*(\mathbf{x}) \psi(\mathbf{x}) + \frac{x}{\beta_G^3} \sum_{\mathbf{x}} [\psi^*(\mathbf{x}) \psi(\mathbf{x})]^2. \quad (2)$$

In Eq. 2 $\alpha_i(\mathbf{x}) = aqA_i(\mathbf{x})$ and $\alpha_{ij} = \alpha_i(\mathbf{x}) + \alpha_j(\mathbf{x} + \hat{i}) - \alpha_j(\mathbf{x}) - \alpha_j(\mathbf{x} + \hat{j})$. β_G and β_2 are related to the continuum parameters x and y and the lattice constant a ,

$$\beta_G = \frac{1}{aq^2} \quad (3)$$

$$\beta_2 = \frac{1}{\beta_G} \left[6 + \frac{y}{\beta_G^2} - \frac{3.1759115(1+2x)}{2\pi\beta_G} - \frac{(-4+8x-8x^2)(\ln 6\beta_G + 0.09) - 1.1 + 4.6x}{16\pi^2\beta_G^2} \right]. \quad (4)$$

Note that β_2 contains the effect of ultraviolet renormalization in the continuum limit when the lattice constant $a \rightarrow 0$ ^{7,26}. The model Eq. 2 is defined on a numerical grid of size $N_x \times N_y \times N_z$, corresponding to a *physical* size of $L_x \times L_y \times L_z$, with $L_i = N_i a$. All our simulations have been on cubic systems with $\beta_G = 1$.

To impose an external magnetic field²⁷, we modify the

action Eq. 2 by changing the field energy along one stack of plaquettes located at x_0, y_0 in such a way that the action is minimized for $\alpha_{12}(x_0, y_0, z) = -2\pi n$ instead of zero, corresponding to forcing a number of n flux quanta through the system. Hence, the action $S[\boldsymbol{\alpha}, \psi; n]$ for n flux-quanta forced through the system, is given by

$$S[\boldsymbol{\alpha}, \psi; n] = S[\boldsymbol{\alpha}, \psi; 0] + \sum_z (2\pi n \alpha_{12}(x_0, y_0, z) + 2\pi^2 n^2). \quad (5)$$

The second term in Eq. 5 corresponds to forcing a flux Φ_B through the lattice in the negative z -direction

$$\frac{\alpha_{12}(x_0, y_0, z)}{q} = a^2 q (\nabla \times \mathbf{A}(x_0, y_0, z))_z = -\frac{2\pi n}{q}. \quad (6)$$

The crucial point is that, due to periodicity, the total flux through the system *must be zero*, i.e.

$$\sum_{x,y} \alpha_{12}(x, y, z) = 0 \quad \forall z.$$

Consequently, the n flux-quanta of the total flux $2\pi n/q$ must return in the $+z$ direction. This flux returns in a manner specified by the dynamics of the theory,²⁷ and it is this *response* which is the topic of interest in the current paper.

The experimental situation corresponds to applying an external magnetic field H , and then study the magnetic response of the superconductor to this field. Hence, a suitable thermodynamic description is coached in terms of a potential $\Phi(H)$, which is a function of the *intensive* field variable H . In the simulations we have fixed n , which is analogous to fixing the magnetic induction, and

a description based on the *extensive* field variable B is more appropriate. The two approaches are related by a Legendre transformation²⁷. In principle the simulations could also be performed in an ensemble with fixed magnetic field. Technically this would be achieved by adding the term

$$HL_z 2\pi n/q$$

to the action in Eq. 1. This would promote n to a dynamical variable of the theory, and be more in accordance with the experimental situation. However, a change $n \rightarrow n \pm 1$ would require a global relaxation, and this would give very low acceptance rates, i.e. inefficient simulations.

For type-I superconductors, superconductivity vanishes for $H > H_c$. For type-II superconductors, a *flux line lattice* is formed at $H = H_{c1}$, for smaller fields the magnetization in the sample vanishes due to the Meissner effect. By fixing n one can not study these effect directly, however it is possible to determine a corresponding field strength from n , see Ref. 27.

On the basis of simulations performed using the modified action Eq. 5, we have determined the *effec-*

tive temperature-renormalized interaction between two vortex-lines, and searched for the value of the GL parameter, or more precisely its square, $x_{I/II}$, where this interaction changes character from being effectively attractive to being effectively repulsive. In section II A we have fixed $n = 2$ and studied the distance between the flux lines. In section II B we have generalized to real n , and used this to calculate a free energy difference between states containing one and two vortices. This is also a measure of the sign of the effective vortex interaction, and hence an indication of whether we have type-I or type-II behavior.

To obtain the results in Figs. 1, 2, and 5 we have performed simulations on cubic systems of size $N = 8, 12, 16, 24, 32, 48$, with $\beta_G = 1.00$. All simulations have been performed in the broken symmetry state $y < y_c$, with particular emphasis on the values $y = -0.04, -0.10, -0.20, -0.30, -0.40$. For the two largest system sizes the final datapoints are averages of approximately 10^6 sweeps, whereas approximately 10^5 sweeps have been performed for the four smallest system sizes.

The simulations leading to the results of Fig. 4 are quite different. They are performed for the fixed system parameters $N = 24$ and $\beta_G = 1.00$, and for each value of m , we have performed from $2.5 \cdot 10^4$ to $2.5 \cdot 10^5$ MC sweeps through the lattice. One sweep through the lattice consists of (1) conventional local Metropolis updates of ψ and \mathbf{A} , and (2) global radial updates of $|\psi|$ combined with overrelaxation^{28,29} of ψ .

A. Effective vortex interaction

We first clarify what is meant by *effective vortex interaction* in this context. In the Ginzburg-Landau model at zero temperature, one may compute a pair-potential between two vortices which consists of an attractive part due to vortex-core overlap, and a repulsive part due to circulation of supercurrents (or magnetic fields) outside the vortex core. Ignoring fluctuation effects, this furnishes an adequate way of distinguishing between type-I and type-II behavior, by asking when the attractive core-contribution dominates the magnetic field contribution or vice versa. By effective interaction, we mean a thermally renormalized pair interaction which fully takes entropic contributions into account. At low temperatures the effective interaction will revert back to the standard pair-interaction described above, but will deviate as temperature is raised, and this is particularly relevant as the critical temperature is approached, as we shall see below. We also comment further on this in the Discussion section, where we elaborate on what we perceive to be a crossover between type-I and type-II behavior.

In our simulations, the value of n has been fixed to $n = 2$. This corresponds to the case of two field-induced vortices which move around in the system under the influence of their mutual effective interaction. During the simulations, we have measured the transverse position

$r_{\perp}(z)$ of these two vortices labelled by 1 and 2, and the average distance between them.

$$\mathbf{d} = \frac{1}{N_z} \sum_z |r_{\perp}^1(z) - r_{\perp}^2(z)|. \quad (7)$$

For type-I superconductors this distance should be independent of system size, whereas for type-II we expect that this distance scales with the system size. Finite size scaling of \mathbf{d} for various points in the (x, y) phase diagram is shown in Fig. 1.

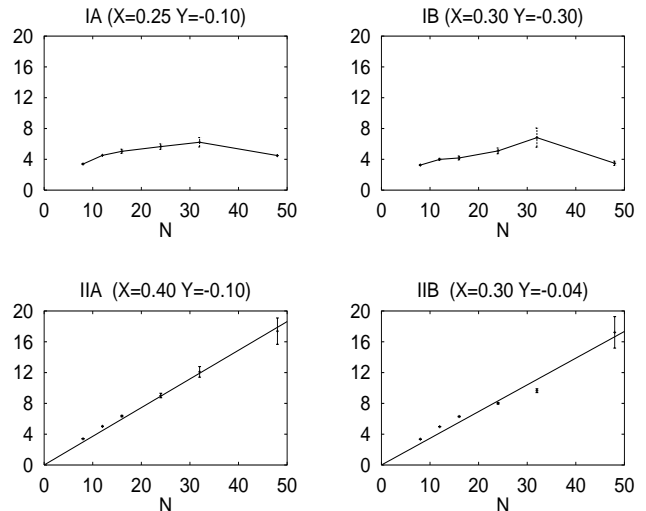


FIG. 1: The ensemble averaged separation $\langle d \rangle$ between the two vortices, as a function of system size. The two upper figures are indicative of type-I behavior, whereas the two lower ones indicate type-II behavior.

In the part of phase diagram which we focus on, namely the region defined by the dotted line in Fig.1 of Ref. 7, the vortex lines are generally directed and almost straight, well defined line objects. This can be seen either by directly taking snapshot pictures of the vortex-line configurations of the system, or by computing the mean-square fluctuations around a straight-line configuration, $\langle |r_{\perp}^i(z) - r_{\perp}^i(0)|^2 \rangle$, for *one* vortex line. This is in contrast to the situation in the vicinity of the *critical* part of $y_c(x)$ in Fig. 1 of Ref. 7, where the vortex lines loose their line tension via a vortex-loop blowout^{12,13}. Consequently, we can consider the theory as an effective theory for an interacting pair of straight vortex lines which interact with the dimensionless potential $V(\mathbf{d})$. If we make this assumption, the probability of finding the vortices separated by a distance \mathbf{d} in a system of N^3 lattice points with *periodic boundary conditions*, is given by

$$P_N(\mathbf{d}) = \frac{e^{-V(\mathbf{d})} \Omega_N(\mathbf{d})}{Z_{\mathbf{d}}}, \quad (8)$$

where $\Omega_N(\mathbf{d})$ is the number of configurations with a transverse vortex-vortex distance of \mathbf{d} , and $Z_{\mathbf{d}}$ is just a

normalisation factor. $\Omega_N(\mathbf{d})$ can be calculated, either analytically in the continuum limit

$$\Omega_N(\mathbf{d}) = \begin{cases} 2\pi\mathbf{d} & \mathbf{d} < \frac{N}{2} \\ 2N \left(\frac{\pi}{2} - 2 \arccos \left(\frac{N}{2\mathbf{d}} \right) \right) & \frac{N}{2} < \mathbf{d} < \frac{N}{\sqrt{2}}, \end{cases} \quad (9)$$

or by simple geometric counting in the case of a lattice. In the case of noninteracting vortices, i.e. $V(\mathbf{d}) = 0$, the expectation value of \mathbf{d} is determined only by $\Omega_N(\mathbf{d})$, and we find the numerical value

$$\mathbf{d}_0 \equiv \langle \mathbf{d} \rangle = \frac{1}{Z_{\mathbf{d}}} \int_0^{\frac{N}{\sqrt{2}}} d\mathbf{d} \Omega_N(\mathbf{d}) \mathbf{d} \approx 0.38N. \quad (10)$$

The separation \mathbf{d}_0 defined in Eq. 10 will be used to establish a numerical value of $x_{I/II}$. Namely, we can compute the averaged distance between vortices at fixed x varying y , or vice versa. In the latter case, we will use the criterion that if $\langle \mathbf{d} \rangle$ exceeds some value $c\mathbf{d}_0$ where c is some fraction, then we have type-II behavior, otherwise it is type-I. The quantity $\langle \mathbf{d} \rangle$ at fixed y will turn out to be an S-shaped curve as a function of x , increasing from small values to large values as x is increased. We interpret this as yet another manifestation of the crossover from type-I to type-II behavior, and we have chosen to locate the crossover region $x_{I/II}$ at the value of x where the curves change most rapidly, which is roughly when $\langle \mathbf{d} \rangle \approx \mathbf{d}_0/2$. As we shall see (see Fig. 6), different crossover criteria give consistent results. The quantity $P_N(\mathbf{d})$ can be estimated from histograms, and then we can use Eq. 8 to determine the pair potential. Depending on whether we consider type-I or type-II superconductors we expect to see an attractive or a repulsive potential. Fig. 2 shows the potential $V(\mathbf{d})$ for the same points of the phase diagram as Fig. 1.

B. Free energy

In Eq. 5 we have used n to indicate an integer number of flux tubes, but in principle there is no reason to limit n to integer values, and we will use $S[\alpha, \psi, m]$ to denote a generalisation to real n .

We have considered the free energy difference between a state containing zero vortices, i.e. $m = 0$ and a state containing n vortices. We can not measure absolute values of the free energy, but by differentiating²⁷

$$e^{-F(m)} = \text{Tr} e^{-S(m)} \quad (11)$$

with respect to m , and then integrating up to n , we can calculate $\Delta F(n) = F(n) - F(0)$,

$$\frac{\Delta F(n)}{L_z q^2} = 2\pi\beta_G \int_0^n dm \left[\underbrace{2m + \frac{1}{\pi N_z} \left\langle \sum_z \alpha_{12}(x_0, y_0, z) \right\rangle_m}_{\equiv W(m)} \right]. \quad (12)$$

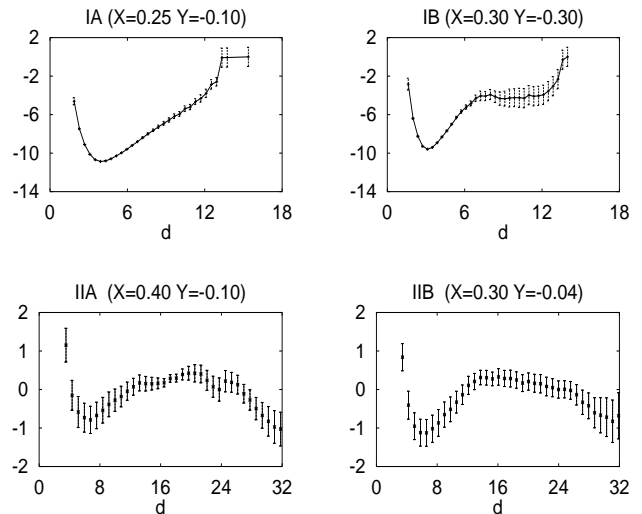


FIG. 2: The effective interaction potential between vortices $V(\mathbf{d})$ as determined from Eq. 8. Observe the difference in vertical scale, in the lower panels (type-II) the interactions are much weaker than in the upper panels (type-I). The graphs correspond to the same points in (x, y) as those in Fig. 1.

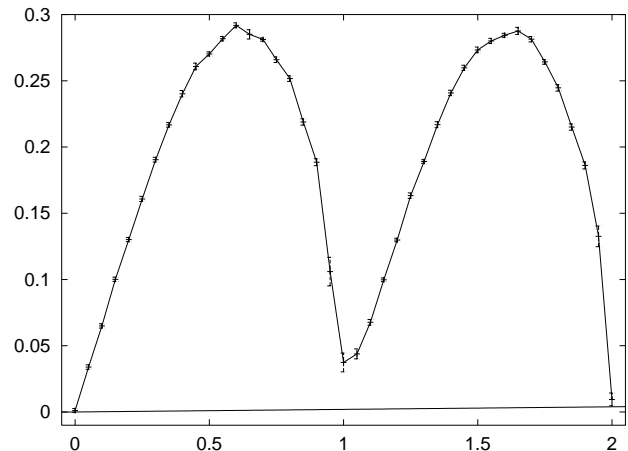


FIG. 3: $W(m)$ The straight line corresponds to $2m/N_x N_y$ which according to Eq. 13 should be satisfied for m integer.

To calculate ΔF , we have then varied m in steps of $\Delta m = 0.05$, and performed the integration in Eq. 12 numerically. Using shift symmetries, it can be shown²⁷ that $W(n)$ is equal to

$$W(n) = \frac{2n}{N_x N_y}, \quad (13)$$

and the behavior for intermediate real values is shown in Fig. 3. Increasing n from 0 to 1 costs a free energy $\Delta F(1)$, and adding two vortices costs an amount $\Delta F(2)$. We will *always* have $\Delta F(2) > \Delta F(1)$, but the question is whether $\Delta F(2) \geq 2\Delta F(1)$. We may regard $F(n+2) + F(n) - 2F(n+1)$ as the discrete second deriva-

tive of the free energy with respect to particle number, which is nothing but the inverse compressibility K^{-1} of the vortex-system. In the thermodynamic limit this quantity can never become negative. However, its vanishing signals the onset of *phase-separation* of the vortex system, which we again interpret as a lack of stability of the vortex-loop tangle, characteristic of type-I behavior.

C. Vortex compressibility, separation, and crossover

We next define a quantity ΔT by the relation

$$\Delta T = \frac{\Delta F(1)}{L_z} - \frac{\Delta F(2)}{2L_z}, \quad (14)$$

which means that ΔT measures the relative free-energy difference between adding one vortex to the system and half of that adding two vortices to the system. Intuitively it is therefore clear that it measures the sign of the vortex interactions, and hence determines whether we are in the type-I or type-II regime. $\Delta T > 0$ signals attractive interactions, i.e. type-I behavior, whereas $\Delta T \leq 0$ signals repulsive interactions, i.e. type-II behavior. We have calculated ΔT by using Eq. 12 and Eq. 14, the results are shown in Fig. 4. The main qualitative result from these simulations is again that $x_{I/II}(y)$ is a declining function of y . Note also that $K^{-1} = -\Delta T$, and hence a positive ΔT clearly implies phase-separation and instability of the vortex system, characteristic of type-I behavior. This is precisely what we see for small x in Fig. 4.

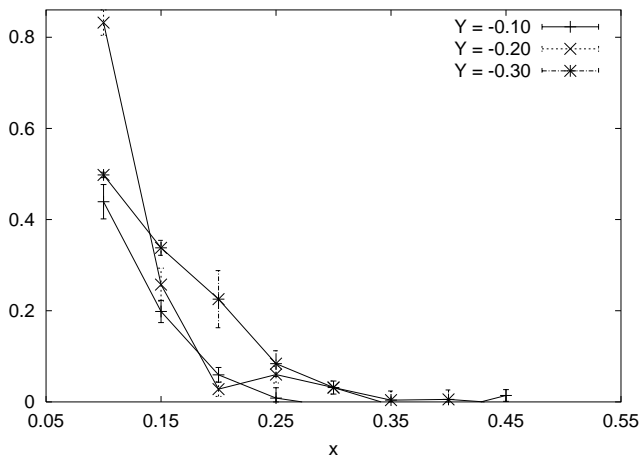


FIG. 4: $\Delta T(x)$ for different values of y . The attraction vanishes for $x_{I/II} < 0.5$, and $x_{I/II}(y)$ is an increasing function of $|y|$.

Finite size scaling of $\langle d \rangle$ and studies of ΔT differentiate nicely between strongly type-I and type-II superconductors, but it is difficult to locate a value of $x_{I/II}(y)$ with any great precision. Fig. 5 shows $\langle d \rangle(x)$ for different values of y , along with a horizontal line at $d_0/2$, where d_0 is the average separation between vortices had they been

non-interacting. We have found that $d_0 \approx 0.38N$ in our simulations. We have, rather arbitrarily, taken the interception of this horizontal line with the curve $\langle d \rangle(x)$ as $x_{I/II}$.

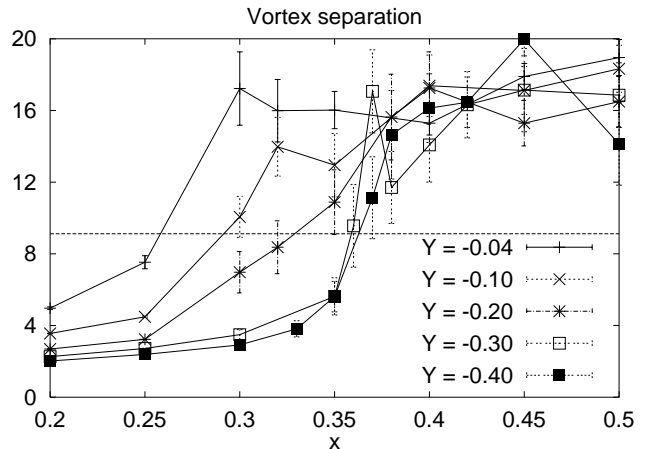


FIG. 5: The ensemble averaged distance between a pair of vortices, $\langle d \rangle$, as a function of the square of the Ginzburg-Landau parameter $x = \kappa^2$, for various values of the temperature-like variable y . The horizontal line is at $d_0/2$. Increasing y amounts to increasing the temperature.

The curves of $\langle d \rangle(x)$ do not get significantly sharper with increasing system size, and there are no particular sharp features in $S[\alpha, \psi, 2]$ as x is increased beyond $x_{I/II}$. Fig. 6 shows the intercepts from Fig. 5. Due to the features in the curves of Fig. 5, and how the results of Fig. 6 are obtained from them, we tentatively conclude that the computed line of Fig. 6, corresponding to the dashed line of Fig. 1 in Ref. 7, is a *crossover* and *not* a phase transition. However, we comment further on this in the concluding section.

As already indicated, there is some arbitrariness in the location of $x_{I/II}(y)$ in Fig. 6, however the four points labelled by (IA, IB) and (IIA, IIB) clearly are in the type-I and type-II regimes, respectively. This is demonstrated in Figs. 1 and 2.

III. DISCUSSION

From Figs. 1 and 2 we conclude that there is a crossover line separating effective attractive vortex interactions from effective repulsive ones, i.e. type-I and type-II. This line can either be crossed by changing x , i.e. IA \rightarrow IIA, or by changing the temperature i.e. IB \rightarrow IIB in Fig. 6. This means that for x values in a suitable range, we can have in principle have a *temperature induced* crossover from type-I to type-II superconductivity. Finally, we note that $x_{I/II}(y)$ deviates significantly from the mean-field value of $x_{I/II} = 0.5$.

Deep in the type-I regime, we find clear evidence of *attractive* interactions. In the type-II regime the repulsive

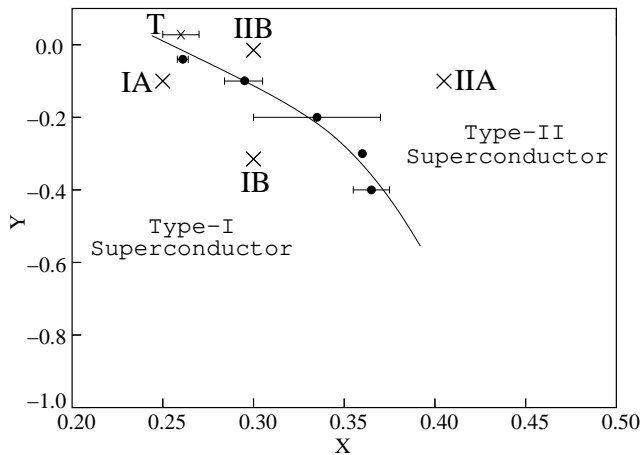


FIG. 6: The computed crossover line $y_{I/II}(x)$ separating type-I and type-II superconductivity. The black circular filled points are given by the intercepts between $d_0/2$ and the curves in Fig. 5. The four points labelled by (IA, IB, IIA, IIB) are the ones that were considered in detail in Figs. 1 and 2. The point marked T is the *tricritical* point in Fig. 1 of Ref. 7, see the discussion of finite size effects in section III A. The solid line connecting the points is *purely* a guide to the eye. The computed line above corresponds to the dotted line of Fig. 1 in Ref. 7 in the vicinity of $(x_{\text{tri}}, y_{\text{tri}})$.

interactions appear to be weak, and the results are essentially also consistent with two *randomly placed* vortex lines, i.e. not interacting, but not consistent with an attractive force between the vortices. Therefore, what the results unequivocally show is that by fixing the material parameter x and varying the temperature-like variable y , the character of the effective pair-potential is altered inside the superconducting regime, significantly away from the critical line.

A. Simulations

The simulations with $n = 2$, and the simulations with a real $m \in [0, 2]$ are quite different, and we will discuss them in turn. An important feature of *all the simulations* in the present work is *slow dynamics*.

For the $n = 2$ simulation, where we have monitored d , we find that deep in the type-I regime the simulations are quite straightforward, the vortices stay close together with only small fluctuations, and a moderate number of sweeps is sufficient to get good statistics. However when we increase x towards $x_{I/II}$ the effect is *not* that d stabilises at a higher value, instead we get fluctuations between a type-I like state where the two vortices are close together, and a type-II like state with large vortex-vortex separation. This picture persists as x is increased into the type-II regime, the only difference is that the fraction of time spent in the type-I like state decreases. In fact the results of Fig. 1 and Fig. 2 are in the type-II region quite close to what we would get from

noninteracting vortices. What makes the simulations difficult is that moving a vortex line in the transverse direction is a *global* change, and thereby very slow. Timeseries of d show characteristic time scales of 10^4 sweeps, so long simulations $\sim 10^6$ sweeps over the lattice are required to obtain acceptable accuracy. A truly high-precision determination of $x_{I/II}(y)$ would surely benefit from a specialized algorithm for the MC updates.

To get good results one should take the $N \rightarrow \infty$ limit. The conclusions from the results of Fig. 1 are based on this limit, whereas those drawn from Figs. 2, 5 and 6 are based on the fixed system size $N = 48$. We have not performed a systematic study of finite size effects, but the curves in Fig. 5 *do have* subject to finite size effects in them. The trend is that curves move to the right upon increasing system size, this very likely explains the apparent discrepancy between the tricritical point (where the $N \rightarrow \infty$ limit has been applied), and the remaining points in Fig. 6.

Note that Eq. 1 is a continuum field theory, and $x_{I/II}(y)$ is *not* a critical point, hence the continuum limit $\beta_G \rightarrow \infty$ should be taken. Our experience from the large-scale simulations performed in Ref. 7 indicates that $\beta_G = 1.00$ provides conditions in the simulations already quite close to the continuum limit. We have therefore chosen to work with $\beta_G = 1.00$ and focused our efforts on considering large systems and long simulations.

The Monte-Carlo computations of ΔT have been even more time consuming, because we have had to do the simulations for 41 different values of m . We have therefore limited ourselves to considering only the system $L = 24, \beta_G = 1.00$, for a discussion of finite N / finite β_G effects see Ref. 27. The relaxation time for these simulations has been particularly long in the limits $m \rightarrow 1^-$ and $m \rightarrow 2^-$, and we therefore have performed much longer simulations in these limits than for intermediate values of m . From Fig. 3 and Eq. 13 it is seen that $W(m)$ is a quantity of order $\mathcal{O}(N^{-2})$ whose finiteness originates in the difference between two $\mathcal{O}(1)$ quantities. Consequently, it is difficult to get numerically precise results. This has in particular been the case in the limits $m \rightarrow 1^-$ and $m \rightarrow 2^-$.

B. Crossover

The physical picture that emerges for the thermal renormalization of the vortex interactions, is the following. At low temperatures, for the κ -values we consider, the system is in the type-I region with a fairly deep minimum in the effective pair-potential between vortices at short distances, leading to an attractive interaction. At very short distances, we find a steric repulsion on the scale of the lattice constants in the system due to the large Coulomb barrier that must be overcome to occupy a link with two or more elementary vortex segments. This length scale represents the size of the vortex core in the problem. Upon increasing the temperature to the vicinity

of the line $y_c(x)$, we do not find large transverse meanderings of the individual vortex lines as we move along each vortex line, rather the vortex lines are essentially straight. Therefore, we believe that it is *not* entropic repulsion due to the bare steric repulsion in the problem, of the type which it seems reasonable to invoke for *strongly* fluctuating elastic strings^{30,31} that renormalizes the vortex interactions in the way that is seen in Fig. 2. Rather, what appears to happen is that the vortex lines slosh back and forth in the minimum of the effective potential well as essentially straight lines. Hence, to a larger and larger extent as temperature is increased, they experience the hard wall in the interactions at small distances, and the weak attraction at large distances, effectively washing out the minimum in the potential, thus making it effectively more repulsive.

This is also seen in our simulations (not shown in any of the figures) when we monitor the transverse meandering fluctuations of each vortex line, $\langle |r_\perp(z) - r_\perp(0)|^2 \rangle$, as well as the mean square fluctuations of the intervortex distance, $\langle d^2 \rangle - \langle d \rangle^2$, where d is defined in Eq. (7). The former is small deep in the superconducting regime, and remains small as the line $y_c(x)$ in Fig. 1 of Ref. 7 is approached, while the latter increases dramatically as the dotted crossover line is crossed. It is precisely this fact which makes the simulations extremely time consuming.

One should however keep in mind that, since we are considering the full GL theory in our simulations, and not the linearized London limit, it is in any case a drastic simplification to view the effective interaction between vortices as a simple pair potential.

Finally, we note that, although our present simulations, which by necessity are on finite-sized systems, indicate that the change from type-I to type-II behavior is a crossover, we cannot rule out the possibility that it is elevated to a true phase-transition in the thermodynamic limit. More work is needed to clarify if this is indeed the case, but this will have to await the next generation of

massive parallel computers. Questions that need to be addressed in this context, are: What is the order parameter of such a transition, and what symmetry, if any, is being broken.

IV. CONCLUSION

We have considered the effective interaction between two vortices in the full GL model, and how this effective interaction is influenced by thermal fluctuations. We have included fluctuations in the gauge fields, as well as the phase- and amplitude-fluctuations of the complex scalar matter field of the problem. We have found that the effective interaction changes from being attractive to being repulsive at $x_{I/II}$. This means a change from type-I to type-II behavior. We have found that $x_{I/II}$ is below the standard quoted value of 0.5, and is a function of the temperature-like parameter y . This means that at the critical point, the value of the GL parameter that separates type-I from type-II behavior is smaller than $1/\sqrt{2}$. The line $x_{I/II}(y)$ appears to be a crossover, and not a true phase transition. The above seems to offer a simple explanation for the experimental observation that elemental Ta and Nb superconductors show a crossover from type-I to type-II behavior as the temperature is increased towards T_c . Previous explanations based on mean-field theories and not involving thermal fluctuations required two additional temperature dependent κ -values to be defined²⁵.

We acknowledge support from the Norwegian Research Council via the High Performance Computing Program (S.M.,J.H.,A.S.), and Grant Nos. 124106/410 (S.M.,A.S.) and 148825/432 (A.S.), and A.S. thanks E. H. Brandt for useful comments. J.H. also acknowledges support from NTNU via a university fellowship.

* Electronic address: Joakim.Hove@phys.ntnu.no

† Electronic address: Sjur.Mo@phys.ntnu.no

‡ Electronic address: Asle.Sudbo@phys.ntnu.no

¹ V. L. Ginzburg and L. D. Landau, Zh. Eksp. Teor. Fiz. **20**, 1064 (1950).

² B. I. Halperin, T. C. Lubensky, and S. K. Ma, Phys. Rev. Lett. **32**, 292 (1974).

³ S. Coleman and E. Weinberg, Phys. Rev. D **7**, 1988 (1973).

⁴ The efforts of Refs. 2 and 3 appear to be among the first to seriously address the principle of emergent order from disorder.

⁵ C. Dasgupta and B. I. Halperin, Phys. Rev. Lett. **47**, 1556 (1981).

⁶ J. Bartholomew, Phys. Rev. B **28**, 5378 (1983).

⁷ S. Mo, J. Hove, and A. Sudbø, Phys. Rev. B **65**, 104501, (2002), [cond-mat/0109260 (2001)].

⁸ H. Kleinert, Lett. Nuovo Cimento **35**, 405 (1982).

⁹ It is customary to describe as tricritical any point in a pa-

parameter space at which a continuous transition becomes discontinuous, irrespective of the number of phases which co-exist along the first-order line or surfaces of critical points which, in a suitably enlarged parameter space may be found to meet here¹⁰.

¹⁰ I. D. Lawrie and S. Sarbach in *Phase Transitions and critical phenomena*, eds C. Domb and M. S. Green, Academic Press, (1984).

¹¹ Had the gauge-field been *massive* it could have been integrated out with impunity to yield an effective $|\phi|^4$ -term, and the theory would yield nicely to renormalization group treatment of the sort that has been successful for Helium IV. In fact, there exists a dual formulation of the three-dimensional Ginzburg-Landau theory which is a new Ginzburg-Landau theory with such a massive gauge-field, see Refs. 7,8,12,13.

¹² Z. Tešanović, Phys. Rev. B **59**, 6449 (1999).

¹³ A. K. Nguyen and A. Sudbø, Phys. Rev. B **60**, 15307

- (1999).
- ¹⁴ J. Hove and A. Sudbø, Phys. Rev. Lett. **84**, 3426 (2000).
- ¹⁵ A. A. Abrikosov, Sov. Phys. JETP **5**, 1174 (1957).
- ¹⁶ H. B. Nielsen and P. Olesen, Nucl. Phys. B **61**, 45 (1973).
- ¹⁷ E. Müller-Hartmann, Phys. Lett. **23**, 521 (1966), *ibid* 619.
- ¹⁸ L. Jacobs and C. Rebbi, Phys. Rev. B **19**, 4486 (1979).
- ¹⁹ L. Kramer, Phys. Rev. B **3**, 3821 (1971).
- ²⁰ E. B. Bogomol'nyi, Sov. J. Nucl. Phys. **23**, 588 (1976).
- ²¹ E. B. Bogomol'nyi, Sov. J. Nucl. Phys. **24**, 449 (1976).
- ²² I. Luk'yanchuk, Phys. Rev. B **63**, 174504 (2001).
- ²³ H. Kleinert and F. S. Nogueira, `cond-mat/0104573`.
- ²⁴ J. Auer and H. Ullmaier, Phys. Rev. B **7**, 136 (1973).
- ²⁵ K. Maki, Physics **1**, 21 (1964); G. Eilenberger, Phys. Rev. **153**, 584 (1967). See also Ref. 24, section III.E.
- ²⁶ M. Laine and A. Rajantie, Nucl. Phys. B **513**, 471 (1998) [`hep-lat/9705003`].
- ²⁷ K. Kajantie, M. Laine, T. Neuhaus, A. Rajantie and K. Rummukainen, Nucl. Phys. B **559**, 395 (1999)[`hep-lat/9906028`].
- ²⁸ K. Kajantie, M. Laine, K. Rummukainen, and M. Shaposhnikov, Nucl. Phys. B **466**, 189 (1996)[`hep-lat/9510020`].
- ²⁹ P. Dimopoulos, K. Farakos and G. Koutsoumbas, Eur. Phys. J. C **16**, 489 (2000)[`hep-lat/9911012`].
- ³⁰ J. Zaanen, Phys. Rev. Lett. **84**, 753 (2000).
- ³¹ S. Mukhin, W. van Saarloos, and J. Zaanen, Phys. Rev. B **64**, 5105 (2001)[`cond-mat/0103253`].